Journal of Medical Imaging

MedicalImaging.SPIEDigitalLibrary.org

Retrospective four-dimensional magnetic resonance imaging with image-based respiratory surrogate: a sagittal–coronal–diaphragm point of intersection motion tracking method

Yilin Liu
Fang-Fang Yin
Brian G. Czito
Mustafa R. Bashir
Manisha Palta
Jing Cai

SPIE.

Yilin Liu, Fang-Fang Yin, Brian G. Czito, Mustafa R. Bashir, Manisha Palta, Jing Cai, "Retrospective four-dimensional magnetic resonance imaging with image-based respiratory surrogate: a sagittal–coronal–diaphragm point of intersection motion tracking method," *J. Med. Imag.* **4**(2), 024007 (2017), doi: 10.1117/1.JMI.4.2.024007.

Retrospective four-dimensional magnetic resonance imaging with image-based respiratory surrogate: a sagittal–coronal–diaphragm point of intersection motion tracking method

Yilin Liu,[a,b] Fang-Fang Yin,[a,b] Brian G. Czito,[b] Mustafa R. Bashir,[b,c] Manisha Palta,[b] and Jing Cai[a,b,*]
[a]Duke University, Medical Physics Graduate Program, Durham, North Carolina, United States
[b]Duke University Medical Center, Department of Radiation Oncology, Durham, North Carolina, United States
[c]Duke University Medical Center, Center for Advanced Magnetic Resonance Development, Durham, North Carolina, United States

Abstract. A four-dimensional magnetic resonance imaging (4-D-MRI) technique with Sagittal–Coronal–Diaphragm Point-of-Intersection (SCD-PoI) as a respiratory surrogate is proposed. To develop an image-based respiratory surrogate, the SCD-PoI motion tracking method is used for retrospective 4-D-MRI reconstruction. Single-slice sagittal MR cine was acquired at a location near the center of the diaphragmatic dome. Multiple-slice coronal MR cines were acquired for 4-D-MRI reconstruction. As a motion surrogate, the diaphragm motion was measured from the PoI among the sagittal MRI cine plane, coronal MRI cine planes, and the diaphragm surface. These points were defined as the SCD-PoI. This point is used as a one-dimensional diaphragmatic navigator in our study. The 4-D-MRI technique was evaluated on a 4-D digital extended cardiac-torso (XCAT) human phantom, a motion phantom, and seven human subjects (five healthy volunteers and two cancer patients). Motion trajectories of a selected region of interest were measured on 4-D-MRI and compared with the known XCAT motion that served as references. The mean absolute amplitude difference (D) and the cross-correlation coefficient (CC) of the comparisons were determined. 4-D-MRI of the XCAT phantom demonstrated highly accurate motion information ($D = 1.13$ mm, CC $= 0.98$). Motion trajectories of the motion phantom measured on 4-D-MRI matched well with the references ($D = 0.54$ mm, CC $= 0.99$). 4-D-MRI of human subjects showed minimal artifacts and clearly revealed the respiratory motion of organs and tumor (mean $D = 1.08 \pm 1.03$ mm; mean CC $= 0.96$). A 4-D-MRI technique with image-based respiratory surrogate has been developed and tested on phantoms and human subjects. [DOI: 10.1117/1.JMI.4.2.024007]

Keywords: four-dimensional magnetic resonance imaging; respiratory motion management; diaphragm surrogate; liver cancer.

Paper 17022R received Jan. 27, 2017; accepted for publication Jun. 1, 2017; published online Jun. 19, 2017.

1 Introduction

Four-dimensional magnetic resonance imaging (4-D-MRI) is a promising technology for motion management in radiation therapy (RT), especially for abdominal applications. Ideally, 4-D-MRI should be achieved using ultrafast three-dimensional (3-D)-MRI sequences for real-time volumetric imaging. However, due to current technical limitations, a significant compromise on image quality has to be made to achieve the high speed of 3-D-MRI.[1,2] Alternatively, 4-D-MRI can be achieved using 3-D-MRI sequences with retrospective k-space sorting. As 3-D-MRI requires a much larger shimming volume relative to two-dimensional (2-D)-MRI, however, inadequate shimming quality is a contributing factor toward the degradation of 4-D-MR image quality.[3] Alternatively, 4-D-MRI can be achieved using fast 2-D-MRI with either prospective gating or retrospective sorting, both of which require a surrogate[4–6] to monitor respiratory motion during image acquisition.

The instability of internal surrogates and the inconvenience of external surrogates have been shown to adversely affect 4-D-MRI.[7–9] This consequently limits clinical implementation. For example, surgically implanted internal biomarkers could migrate in a subject's body, decreasing the validity of the correlation between the surrogates with the motion of tumor.[7] External surrogates usually required a prescan setup, increasing the complexity of the MRI scan. Image-based surrogate techniques, such as the body area (BA) surrogate developed by Cai et al.,[5] may be subject to error due to its weak signal from the respiratory motion in the anterior–posterior direction. To increase the signal of the surrogate, the use of the superior–inferior (SI) respiratory motion is preferred. The diaphragm has been shown to be a reasonable internal surrogate as it (1) captures motion in the SI direction, (2) demonstrates internal respiratory motion, and (3) can be readily extracted from 2-D-MRIs due to the well-defined edge between liver and lung tissue.

This study aims to investigate the feasibility of developing a retrospective 4-D-MRI technique with an image-based respiratory surrogate, using the sagittal–coronal–diaphragm point of intersection (SCD-PoI) diaphragm motion. Compared with other respiratory surrogates, this new surrogate has the potential to provide a more accurate and reliable breathing signal for

*Address all correspondence to: Jing Cai, E-mail: jing.cai@duke.edu

2329-4302/2017/$25.00 © 2017 SPIE

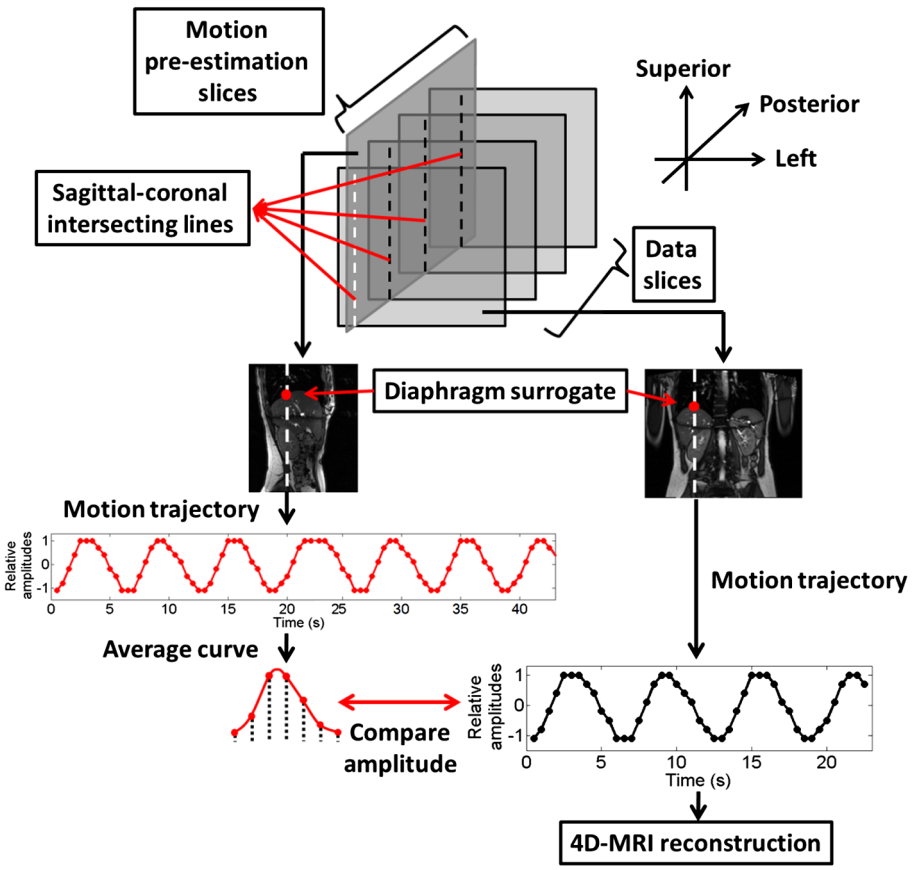

Fig. 1 Workflow of 4-D-MRI using SCD-PoI as the respiratory surrogate.

4-D-MRI applications. The proposed SCD-PoI method was evaluated and validated on a 4-D digital extended cardiac-torso (XCAT) human phantom,[10] a physical motion phantom, and human subjects.

2 Methods and Materials

2.1 *Four-Dimensional Magnetic Resonance Imaging Technique Using the Sagittal–Coronal–Diaphragm Point of Intersection Respiratory Surrogate*

Image acquisition of the proposed 4-D-MRI technique using the SCD-PoI respiratory surrogate consists of two steps. First, a fast imaging technique that employs steady-state acquisition[11,12] [FIESTA in gradient echo (GE) and TrueFISP in Siemens] was employed to acquire single-slice sagittal cine images near the center of the diaphragm for 1 to 2 min. This is performed to estimate the average breathing cycle of the subject. Second, the FIESTA/TrueFISP MR sequence was used to acquire cine images in the coronal plane at multiple-slice locations covering the entire volume of interest. The imaging time at each slice location was slightly longer than the breathing period. The multiple-slice coronal cine images were retrospectively sorted using the method described below to reconstruct the 4-D-MRI.

The intersecting lines of the sagittal planes and the coronal planes were labeled sagittal–coronal intersecting lines (SCL) in this study. The PoI of each SCL with the diaphragm was tracked as a surrogate for respiratory motion as shown in Fig. 1. The PoI of the diaphragm with each SCL is labeled SCD-PoI.

Each coronal slice location has an associated SCL on the sagittal cine. A motion trajectory of the SCD-PoI can be extracted from the sagittal cine as shown in Fig. 1. Subsequently, the average breathing curve of the motion trajectory is determined; it is then divided into respiratory phases. The motion amplitude range on the average respiratory curve was determined as the reference of the motion amplitude range for each phase. Meanwhile, as the SCL can also be observed on the coronal cine at the corresponding slice location, the same SCD-PoI can also be tracked on the coronal cine, as shown with the black curve on the right side of Fig. 1. Each dot on the curve represents one 2-D image from the coronal cine at one example slice location. With the diaphragm motion amplitude information determined for each 2-D image of the coronal cine, the amplitudes were compared with the reference of the motion amplitude range for each phase bin. Amplitude sorting was conducted for each of the 2-D coronal cine images to select images for each respiratory bin. As the amplitude reference range was determined based on respiratory phases from the average breathing curve, the sorting process was labeled phase sorting, and each respiratory bin was labeled a phase bin. In our study, the total number of phase bins was set to be 6. This process was repeated for each coronal cine slice location to generate the 4-D-MRI.

If there was more than one image to choose from for a particular phase, the most representative frame with minimum amplitude error as compared with the average breathing curve was used. The image nearest the adjacent bin at the same slice location was used in the event that any individual phase was missing image information.

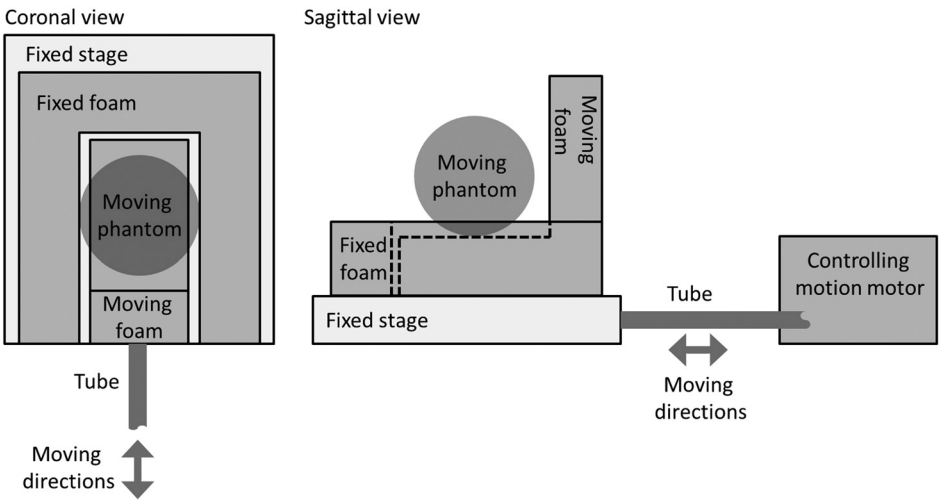

Fig. 2 Illustration of the structure of the motion phantom and its setup in the experiment.

2.2 *Digital Phantom Study*

The proposed 4-D-MRI technique was first tested on the 4-D-XCAT digital human phantom,[10] and motion was controlled by a regular breathing cycle. XCAT images were generated with the following parameters: 256×100, voxel size: 2.5×3 mm, slice thickness: 5 mm, maximum diaphragm motion: 30 mm, maximum anterior body motion: 10 mm, breathing period: 5 s, and frames rate: 5 frames/s. An artificial spherical tumor (diameter: 30 mm) was inserted into the liver of the phantom to move concurrently with the surrounding tissue.

Virtual experiments of the proposed 4-D-MRI technique were carried out on the 4-D-XCAT phantom as follows: (1) volumetric data sets of the phantom were generated at the same frame rate as the MR sequence (e.g., 5 frames/s), (2) MR image acquisition was mimicked for the single-slice sagittal cine and multiple-slice coronal cine by extracting 2-D images from the volumetric XCAT volumes, (3) motion of the diaphragm at SCD-PoI on sagittal cines and coronal cines was tracked. To validate the SCD-PoI as a respiratory surrogate, the breathing signal determined based on SCD-Pol was compared with the input breathing signal, (4) average breathing pattern was estimated from the single-slice sagittal cine, and (5) breathing signals were determined based on SCD-PoI from multiple-slice coronal cine images. Finally, we sorted the coronal images by comparing the estimated motion amplitude range of each phase and the SCD-PoI motion amplitude of each coronal cine image to generate the 4-D-MRI.

To evaluate the simulated "4-D-MRI," tumor motion trajectory in the SI direction measured from the 4-D-MRI was compared with the average breathing curve of the input signal. Mean absolute amplitude difference (D) and cross-correlation coefficient (CC) between the two curves were measured.

2.3 *Motion Phantom Study*

The proposed 4-D-MRI technique was then tested on an in-house constructed MRI-compatible motion phantom whose motion was controlled by a motor via a rigid tube. Figure 2 shows the structure of the phantom. Figure 3 shows an actual motion phantom and its setup in the MR scanner. The motion stage consists of a supporting platform (2-cm solid water slab) and a small gel (to simulate the motion of liver). The phantom gel that was placed on the motion stage in Fig. 3 is an irregular shape gel, simply to demonstrate that the motion stage can carry any shape of phantom gel. In the MR scan, in this study, we used a spherical phantom taped on the motion stage. A sinusoid curve with peak-to-peak amplitude of 15 mm and period of 4 s was used in this study. The superior half of the phantom edge perpendicular to the motion direction was used to mimic the motion of the diaphragm.

Fig. 3 Illustration of motion phantom and its setup in the MR scanner.

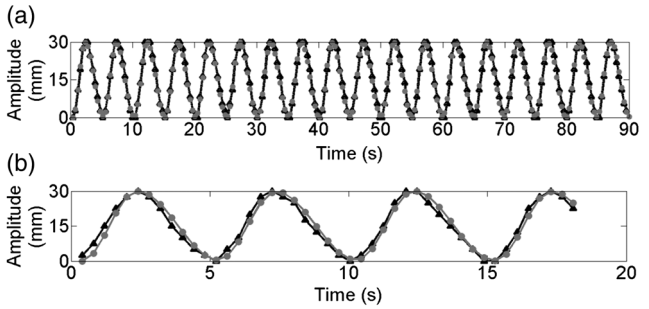

Fig. 4 (a) Breathing signals (black curve with triangles) extracted using SCD-PoI from single-slice sagittal cine and (b) one slice of multiple-slice coronal cine. Both of the signals matched well with the input breathing profile (gray curve with circles).

MR images were acquired on a GE 1.5T system using the FIESTA sequence with head coil. Single-slice sagittal cine and multiple-slice coronal cine were acquired with the following parameters: repetition time/echo time: 3.227 ms/1.0 ms, pixel size: 1.17×1.17 mm, field of view (FOV): 300×300 mm, flip angle: 50 deg, and matrix: 256×256. Slice thickness was 3 mm for the sagittal images and 5 mm for the coronal images. Frame rate was ~3 frames/s. The images were acquired with cine image acquisition mode, not in interleave image acquisition mode. Sagittal cine was acquired for 60 s, and each slice of coronal cine was imaged for 9 s. 6-bin 4-D-MRI images were reconstructed based on the method described earlier. Additional 3-D-volumetric MRI images were acquired using the FIESTA sequence for the water phantom when it was in a static state, which served as a reference for the phantom shape.

To evaluate 4-D-MRI, additional single-slice sagittal cine MR images were acquired at the center of the phantom, providing ground truth of phantom motion for comparison. Motion trajectories of the phantom were determined from 4-D-MRI and compared with those determined from the sagittal cine MR images. D and CC were calculated to quantitatively evaluate the 4-D-MRI image quality.

2.4 *Human Subject Study*

The proposed 4-D-MRI technique was tested on five healthy volunteers (three males and two females, mean age of 30 years) and two cancer patients (one male and one female, mean age of 65 years) in an institutional review board-approved study. MR images were acquired on either a Siemens 3T scanner or a GE 1.5T scanner using a TrueFISP/FIEST sequence with similar parameters as those in the phantom study. All subjects were positioned head-first-supine with arms down with no immobilization device. Single-slice sagittal cine MR using TrueFisp/FIESTA were acquired across the region of interest (ROI), which is the center of the tumor for patients and the center of a hepatic vessel for healthy subjects. To evaluate 4-D-MRI, motion trajectories of the ROIs in the SI direction were determined from 4-D-MRI and compared with those tracked on the single-slice sagittal cine MR images. D and CC were calculated to quantitatively evaluate the 4-D-MRI image quality.

3 Results

3.1 *Validation Study*

Figure 4(a) shows the respiratory signals of the 4-D-XCAT phantom determined from sagittal cine using SCD-PoI and its comparison with the input breathing profile. The mean absolute amplitude difference (±standard deviation) is 1.18 (±0.84) mm. Also, the respiratory signal from one slice of coronal cine is shown in Fig. 4(b) in comparison with the input profile. The mean absolute amplitude difference (±standard deviation) is 1.73 (±1.12) mm.

3.2 *Digital Phantom Study*

Simulated "4-D-MRI" of the XCAT phantom demonstrates highly accurate respiratory motion as shown in Fig. 5(a). No apparent artifacts were observed. Figure 5(b) shows that the tumor motion trajectory in the SI direction demonstrated on 4-D-MRI matches well with the average breathing curve calculated from the input motion profile; D is 1.13 mm and CC is 0.98.

3.3 *Motion Phantom Study*

Figure 6(a) shows the 6-bin 4-D-MRI reconstruction results of the water phantom in axial and sagittal planes, reconstructed from the originally acquired coronal images. The reference images are shown at the same phantom slice locations as those of the 4-D images. Motion is clearly observed with minimal image artifacts on the reconstructed images. Motion trajectories extracted on 4-D-MRI of the motion water phantom matches well with the motion reference ($D = 0.54$ mm, CC = 0.99) as shown in Fig. 6(b).

3.4 *Human Subject Study*

Figure 7 shows the results of a representative healthy volunteer (a, b) and a representative cancer patient (c, d). Minimal artifacts were observed in the 4-D-MRI images with adequate motion information demonstrating both organ and tumor respiratory motion. Motion trajectories of the ROI determined from 4-D-MRI

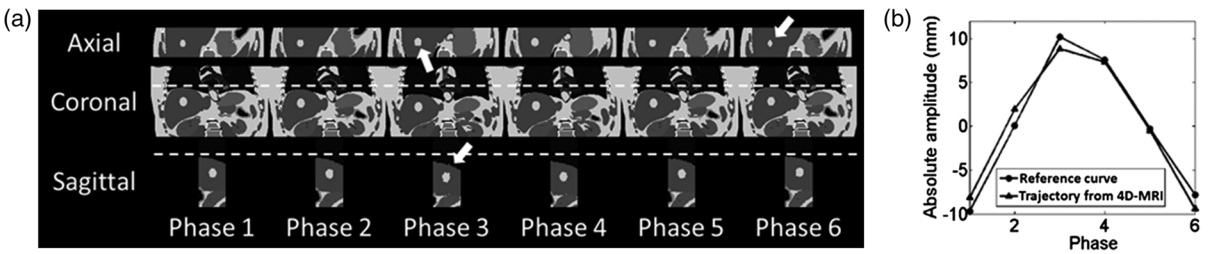

Fig. 5 (a) Simulated 6-bin "4-D-MRI" images and (b) comparison of breathing curves between the 4-D-MRI and the input breathing for the 4-D-XCAT phantom.

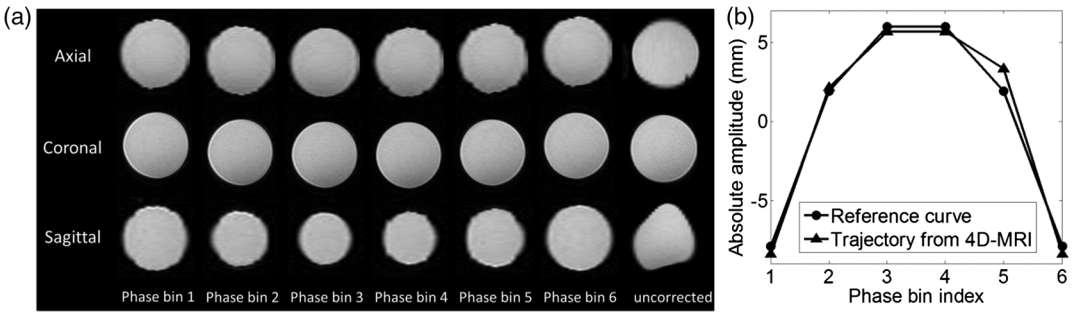

Fig. 6 (a) Six-phase 4-D-MRI images, with uncorrected images as comparison and (b) comparison of phantom motion trajectories between 4-D-MRI and reference cine MR for the MR-compatible motion phantom.

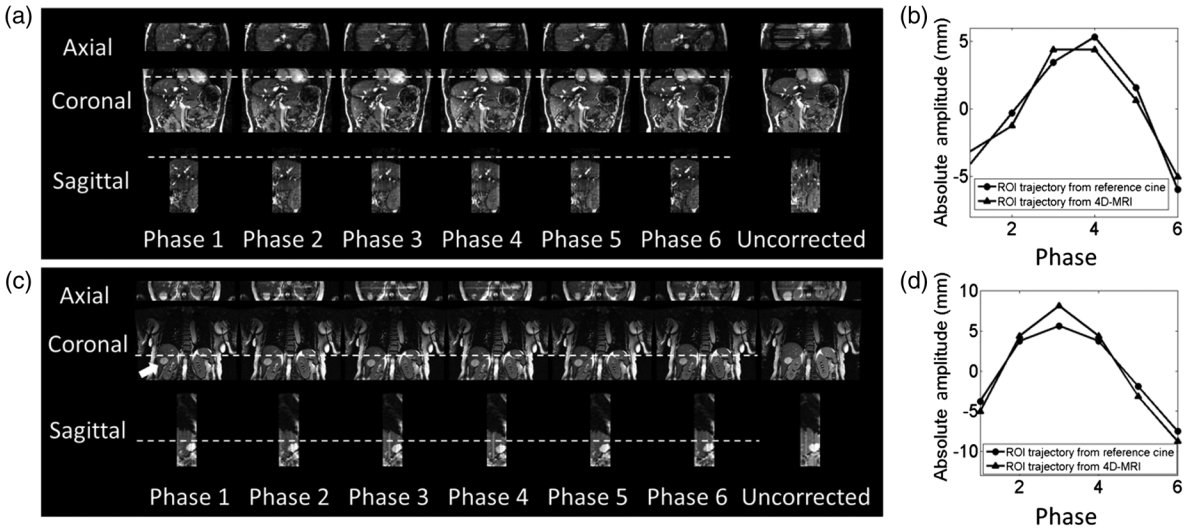

Fig. 7 (a) Six-phase 4-D-MRI images, with uncorrected images as comparison and (b) comparison of ROI motion trajectories between 4-D-MRI and reference cine MR for a representative healthy volunteer. (c) Six-phase 4-D-MRI images (white arrow points out a cyst in liver), with uncorrected images as comparison and (d) comparison of ROI motion trajectories between 4-D-MRI and reference cine MR for a representative cancer patient. A benign cyst in the liver is pointed out by the white arrow.

matched well with those from the reference cine MRI. On average of all subjects, the mean (±standard deviation) D is 1.08 (±1.03) mm and CC is 0.96 (±0.05) in the SI direction.

4 Discussion

4-D-MRI has been shown to be a promising technique for tumor motion management in RT, especially for abdominal cancers. Various approaches have been taken by researchers in the development of 4-D-MRI. For example, Blackall et al.[2] implemented a T1-weighted 3-D real-time MRI using a fast field echo-echo planar imaging sequence with sensitivity encoding parallel acceleration. It achieved a high frame rate (330 ms/volume) and spatial resolution (1.8 mm × 1.8 mm × 7 mm). However, significant compromises in image quality have to be made to achieve real-time imaging, resulting in inadequate image quality for RT application. Hu et al.[6] developed a prospective T2-weighted 4-D-MRI technique with a respiratory amplitude-based triggering system to gate 2-D-MRI image acquisition. In addition, Akçakaya et al.[13] developed a T1-weighted 4-D-MRI k-space-dependent respiratory gating technique. With this technique, a respiratory navigator is used as the surrogate to gate the acquisition of the k-space center data. Both techniques acquire data only when respiratory motion reaches a preset motion amplitude using prospective gating. Cai et al.[5,14] proposed a T2/T1-weighted 4-D-MRI phase sorting technique that used BA extracting from images as the respiratory surrogate for sorting. Tryggestad et al.[15] and Liu et al. separately developed a T2-weighted 4-D-MRI phase sorting technique for a sequential MRI image acquisition mode with an external respiratory surrogate physiologic monitoring unit system. In addition, Liu et al.[16] also implemented a retrospective reordering of k-space based on respiratory phase to generate T2-weighted 4-D-MRI. In summary, 4-D-MRI techniques that have been reported so far have utilized both prospective and retrospective approaches, and have utilized different contrast mechanisms (T1-, T2/T1-, and T2-weighted) and respiratory surrogates (BA, physiologic monitoring unit, k-space center, etc.). Each technique has its own pros and cons, and the full potential for clinical application is yet to be determined. At present, there is no established 4-D-MRI technique that is widely adapted in the radiation oncology clinic.

The 4-D-MRI technique with SCD-PoI surrogate provides an alternative for 4-D-MRI imaging using a convenient, image-based respiratory surrogate. Compared with other techniques,

it utilizes commercially available MR sequences for image acquisition, illuminating the requirement for MR pulse sequence development. It accelerates and simplifies the image acquisition process of 4-D-MRI by imaging in the coronal plane and provides a more accurate breathing signal by extracting respiratory motion in the dominant motion direction of the diaphragm (i.e., the SI direction). As a result, 4-D-MRI with SCD-PoI respiratory surrogate may reduce the respiratory signal vibration noises and increase the signal-to-noise ratio of the respiratory signal.

The difference between external respiratory surrogates and the internal motion of the subject[17] is an important problem in the 4-D imaging field. One of the advantages of the technique we introduced is that it tracks the internal motion of the human subjects. There should be better correlation between the respiratory signals and the internal motion. Furthermore, respiratory motion patterns may vary from slice to slice. Liu et al.[5] described the problem of the space-dependent phase shift in the SI direction, which may occur at different slice locations, in their study using BA as the respiratory surrogate for 4-D-MRI. This is an important concern for most 4-D-MRI studies. In our study, neither the preestimation respiratory signals (extracted from sagittal cine) nor the sorting respiratory signals (extracted from coronal cines) are extracted from images acquired in the axial plane. This obviates the problem of the space-dependent phase shift in the SI direction.

This method is also different from using an MR navigator as the respiratory surrogate. For example, compared with the method of using the navigator to measure respiratory motion as in Von Siebenthal et al.'s study,[18] our method differs in several aspects: (1) the image acquisition schemes are different. Von Siebenthal et al. used an alternate scheme to acquire the navigator and data images, whereas we acquired coronal cine MRI continuously for 4-D reconstruction; (2) the breathing signal generated using SCD-PoI method is self-synchronized, whereas the signal provided by the navigator is not. In Von Siebenthal's study, there is a time interval between the image acquisition of the navigator and the image data. Our method minimized the error that the unsynchronized respiratory signal may cause; (3) the total image acquisition time is different. Acquisition of the navigator slices in between 4-D data images doubled the total imaging acquisition time as compared with that in our method; (4) the 4-D reconstruction methods are different. Von Siebenthal et al. used the frame similarity measurement step before the 4-D reconstruction to deal with the time interval between the navigator and the data image. This step may introduce errors and increases the complexity of the technique. In our study, this step is not required because our respiratory signal is self-synchronized, i.e., self-navigated; and (5) internal motion may have different motion patterns at different locations. In our study, this space-dependent phase shift was corrected in the lateral direction by preestimating respiratory motion pattern at different coronal cine slice locations using sagittal cine, whereas the space-dependent phase shift problem was not considered in Von Siebenthal's study.

There are several limitations in the current study. First, with SCD-PoI as the respiratory motion surrogate, the range of coronal slices locations are limited to the area covered by the dome of the diaphragm in the anterior–posterior direction. For regions near the chest wall or the spinal cord, where motion of the diaphragm may not be observed in the FOV, SCD-PoI probably cannot be used. However, 4-D-MRI focuses on the imaging of abdominal regions, where tumor-tissue contrast is often poor compared with other image modalities, such as 4-D-CT. Almost all organs of interest in RT studies, such as the liver, pancreas, and kidney, can be well observed using this 4-D-MRI technique. Second, the 4-D-MRI image quality can be affected by the native image resolution and slice thickness. Ideally, better image resolution will lead to more accurate motion tracking and thus breathing signal. However, in practical applications, these parameters have to be set in consideration of the total image acquisition time. Third, the postprocessing time is controlled to be in order of minutes (about 5 min, also depend on the data size for each subject) for the whole sorting and image reconstruction process. It may be improved to be in order of seconds with parallel computation. Fourth, only a limited number of regular breathing signals was tested in our phantom studies. The performance of the proposed technique may be affected by the motion amplitude and motion variations, warranting a more comprehensive evaluation with a large number of regular and irregular breathing signals to fully understand its limitations and impacting factors. This is a topic of interest for our future investigation. In addition, the current study that we are presenting is a feasibility study for this technique. It is in the early stage of development. It is possible that we can conduct statistical analysis with more human subject data in our future work.

5 Conclusion

A 4-D-MRI technique with an image-based SCD-PoI respiratory surrogate has been developed and evaluated in a digital phantom, a motion phantom, and human subjects. Compared with other 4-D-MRI techniques, this technique simplifies the 4-D-MRI image acquisition process and can potentially increase the accuracy of 4-D-MRI by reducing the phase-shifting effect.

Disclosures

The authors have no relevant conflicts of interest to disclose.

Acknowledgments

This work is partly supported by funding from the National Institutes of Health (1R21CA165384)

References

1. J. Dinkel et al., "4D-MRI analysis of lung tumor motion in patients with hemidiaphragmatic paralysis," *Radiother. Oncol.* **91**, 449–454 (2009).
2. J. M. Blackall et al., "MRI-based measurements of respiratory motion variability and assessment of imaging strategies for radiotherapy planning," *Phys. Med. Biol.* **51**, 4147–4169 (2006).
3. Z. Deng et al., "Four-dimensional MRI using three-dimensional radial sampling with respiratory self-gating to characterize temporal phase-resolved respiratory motion in the abdomen," *Magn. Reson. Med.* **75**(4), 1574–1585 (2016).
4. Y. Liu et al., "Four dimensional magnetic resonance imaging with retrospective k-space reordering: a feasibility study," *Med. Phys.* **42**(2), 534–541 (2015).
5. J. Cai et al., "Four-dimensional magnetic resonance imaging (4D-MRI) using image-based respiratory surrogate: a feasibility study," *Med. Phys.* **38**(12), 6384–6394 (2011).
6. Y. Hu et al., "Respiratory amplitude guided 4-dimensional magnetic resonance imaging," *Int. J. Radiat. Oncol. Biol. Phys.* **86**(1), 198–204 (2013).
7. N. Kothary et al., "Safety and efficacy of percutaneous fiducial marker implantation for image-guided radiation therapy," *J. Vasc. Int. Radiol.* **20**(2), 235–239 (2009).
8. Y. Tsunashima et al., "Correlation between the respiratory waveform measured using a respiratory sensor and 3D tumor motion in gated radiotherapy," *Int. J. Radiat. Oncol. Biol. Phys.* **60**, 951–958 (2004).

9. N. Bhagat et al., "Complications associated with the percutaneous insertion of fiducial markers in the thorax," *Cardiovasc. Int. Radiol.* **33**, 1186–1191 (2010).
10. W. P. Segars et al., "Realistic CT simulation using the 4D XCAT phantom," *Med. Phys.* **35**, 3800–3808 (2008).
11. C. Plathow et al., "Analysis of intrathoracic tumor mobility during whole breathing cycle by dynamic MRI," *Int. J. Radiat. Oncol. Biol. Phys.* **59**, 952–959 (2004).
12. J. Cai et al., "Evaluation of the reproducibility of lung motion probability distribution function (PDF) using dynamic MRI," *Phys. Med. Biol.* **52**, 365–373 (2007).
13. M. Akçakaya et al., "Free-breathing phase contrast MRI with near 100% respiratory navigator efficiency using k-space-dependent respiratory gating," *Magn. Reson. Med.* **71**(6), 2172–2179 (2014).
14. J. Cai et al., "Investigation of sliced body volume (SBV) as respiratory surrogate," *J. Appl. Clin. Med. Phys.* **14**(1), 71–80 (2013).
15. E. Tryggestad et al., "Respiration-based sorting of dynamic MRI to derive representative 4D-MRI for radiotherapy planning," *Med. Phys.* **40**(5), 051909 (2013).
16. Y. Liu et al., "T2-weighted four dimensional magnetic resonance imaging with result-driven phase sorting," *Med. Phys.* **42**(8), 4460–4471 (2015).
17. H. Fayad et al., "Technical note: correlation of respiratory motion between external patient surface and internal anatomical landmarks," *Med. Phys.* **38**(6), 3157–3164 (2011).
18. M. Von Siebenthal et al., "4D MR imaging of respiratory organ motion and its variability," *Phys. Med. Biol.* **52**(6), 1547–1564 (2007).

Yilin Liu received her PhD in medical physics from Duke University in 2016. She is a medical physics resident at the University of Texas MD Anderson Cancer Center. Her current research interests include application of MRI on radiation therapy, medical image processing, and 4-D imaging. She is a member of AAPM and ISMRM.

Biographies for the other authors are not available.